Spectroscopic properties of Er^{3+}-doped and Er^{3+}/Yb^{3+}-codoped PbF$_2$–MOx (M = Te, Ge, B) oxyfluoride glasses

Zhengang Shang [a,b], Guozhong Ren [a,b,*], Qibin Yang [a,b], Changfu Xu [a],
Yunxin Liu [a], Yong Zhang [a], Qun Wu [a]

[a] *Institute of Modern Physics, Faculty of Material & Photoelectric Physics, Xiangtan University, Xiangtan 411105, China*
[b] *Key Laboratory of Low Dimensional Materials & Application Technology of Ministry of Education, Xiangtan University, Xiangtan 411105, China*

Abstract

A series of Er^{3+}-doped and Er^{3+}/Yb^{3+}-codoped lead germanate (GP), lead tellurite (TP) and lead borate (BP) transparent oxyfluoride glasses were synthesized. Spectroscopic characteristics of these materials were systemically measured. The Judd–Ofelt parameters were calculated according to absorption spectra. F^{-} ions have a strong effect on refractive index (n) and phonon energy of the host. Intense red and green upconversion is closely related to phonon energy, J–O parameters and sensitizer. The GPEY-2 glass (53GeO$_2$–43PbF$_2$–0.5Er$_2$O$_3$–2Yb$_2$O$_3$) shows good transparency and fairly strong upconversion emissions.
© 2007 Elsevier B.V. All rights reserved.

Keywords: Laser materials; Luminescence; Absorption; Raman spectra

1. Introduction

In recent years, the upconversion process of rare-earth ions under infrared laser diode (LD) excitation in transparent hosts has been studied extensively due to potential applications in the fields such as 3D display, optical data storage, under-sea optical communications, biomedical diagnostics, sensors as well as room temperature infrared pumped visible lasers [1–6]. It is well known that Er^{3+} is the most commonly used as an activator among the rare-earth ions [1–4,7–13]. When a rare-earth ion is chosen as the activator of an upconversion material, the host composition becomes a critical factor to be designed since its spectroscopic properties depend strongly on the local environment of hosts [5,14,15]. The research for excellent hosts still attracts much attention of scientists. At present, heavy metal oxyfluoride glass [4,11,16] is considered to be one of the most promising materials because it can combine well good optical, mechanical and thermal-stable properties of the oxides with lower phonon energy of fluorides which can effectively reduce multiphonon decay of excited states in rare-earth ions and thus enhance the optical quantum efficiency [10,17,18].

In this paper, we try to develop upconversion materials being aimed at the application for all-solid-state laser. Although ZBLAN is a good candidate for this purpose it consists of complete fluorides [19,20]. To improve the mechanical, thermal-stable and transparency properties we have designed a series of oxyfluoride materials. Some of them measured not only very transparent but also emit fairly strong green and red lights. With further improvement, we think these materials might be potential solid-state laser materials.

2. Experimental methods and procedure

Glasses were prepared from germanate oxide (GeO$_2$, 99.999%), tellurite oxide (TeO$_2$, 99.9%), borate oxide (B$_2$O$_3$, 99.9%), lead fluoride (PbF$_2$, 99.9%), ytterbium oxide (Yb$_2$O$_3$, 99.99%) and erbium oxide (Er$_2$O$_3$, 99.99%) powders provided from SCRC (Sinopharm Chemical Reagent Co. Ltd.). Compositions of glasses are listed in Table 1. The raw materials were grounded in an agate mortar by hand for at least 1 h. The fully homogeneous powders were then melted by a silicon-carbide furnace in an alumina crucible at 1000 °C (tellurite glasses), 1150 °C (germanate glasses) or 900 °C (borate glasses) for 20 min. The crucibles were covered with alumina lids to reduce volatilization loss. When the melting was completed, the glass liquids were quenched by being rapidly poured onto a stainless steel mold which was preheated in a furnace for 10 min at temperatures of 200–300 °C to prevent from cracking. The glasses were subsequently annealed

* Corresponding author at: Faculty of Material & Photoelectric Physics, Xiangtan University, Xiangtan 411105, China. Tel.: +86 732 8292 113.
E-mail address: rgz76@sohu.com (G.Z. Ren).

Table 1
Composition of the glasses prepared and the RRG $r(i)$

Sample	Composition (mol%)	$r(i)$
1. TPE	$50TeO_2–50PbF_2–0.5Er_2O_3$	0.29
2. TPEY-1	$50TeO_2–50PbF_2–0.5Er_2O_3–1Yb_2O_3$	0.43
3. TPEY-2	$50TeO_2–50PbF_2–0.5Er_2O_3–2Yb_2O_3$	0.93
4. GPE	$53GeO_2–47PbF_2–0.5Er_2O_3$	0.28
5. GPEY-1	$53GeO_2–47PbF_2–0.5Er_2O_3–1Yb_2O_3$	0.75
6. GPEY-2	$53GeO_2–47PbF_2–0.5Er_2O_3–2Yb_2O_3$	1.07
7. BPE	$20B_2O_3–80PbF_2–0.5Er_2O_3$	None
8. BPEY-2	$20B_2O_3–80PbF_2–0.5Er_2O_3–2Yb_2O_3$	1.24

Note: The "x" in TPEY–x ($x = 1, 2$) stands for the concentration of Yb_2O; others follow.

at 300 °C (for tellurite and germanate glasses) or 200 °C (for borate glass) for 1 h, then cooled to room temperature in air and finally sliced and polished for the optical measurement.

Optical absorption spectra in the ultraviolet, visible and near infrared regions were measured with a spectrophotometer (Shumandzu\UV\3101PC). The refractive indexes were measured by a Spectroscopic ellipsometer (Jobin Yvon UVISEL) with the results listed in Table 2. The Raman spectra were recorded on a FT Raman spectrophotometer within the range of 100–1300 cm^{-1} operating at 488 nm argon laser. The upconversion spectra within the range of 12 000–20 000 cm^{-1} were obtained with an R-500 spectrophotometer under the excitation of 980 nm LD. All measurements were taken at room temperature.

3. Results and discussion

Fig. 1 shows the absorption spectra of Er^{3+}-doped glasses. The transparency in GPE glass is 80% calculated by its absorption coefficient, which is the best transparence among all the prepared glasses. The absorption bands are attributed to the transitions from the ground state $^4I_{15/2}$ to the excited states of Er^{3+} ion. The radioactive transitions within $4f^n$ configuration of rare-earth ion can be analyzed by the Judd–Ofelt approach [21,22]. The Judd–Ofelt intensity parameters Ω_λ were calculated by using a least squares fitting approach based on the principle of the electric-dipole contributions of the experimental oscillator strengths. The results are also listed in Table 2 [23,24]. The parameter Ω_2 is considered to be a measure of the degree of co-valency of the chemical bonds between Er^{3+} and its nearest-neighboring atoms. The electro-negativity of O atom is less than that of F atom and thus Ω_2 in BPE is the smallest among the three samples because of its large content of PbF$_2$. Since the Ge–O bonds are more co-valent than the Te–O bonds, the ability donating electron of O^{2-} to Er^{3+} ion can be stronger in TPE glass than that in the GPE glass. The co-valency of chemical bond between the Er^{3+} and the ligand varies with the compo-
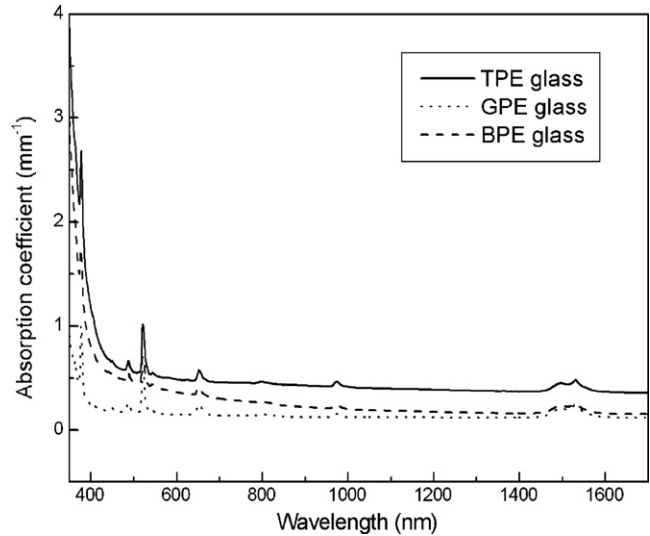

Fig. 1. Absorption spectra for Er^{3+} glasses.

sitions; TPE > GPE > BPE which is confirmed by the values of Ω_2 in Table 2. The parameter Ω_6 is considered to increase with decreasing the "rigidity" of hosts which refers to the mean force constant of Er^{3+}-anion bonds. It is obvious that the value of Ω_6 in oxyfluorides is (see the last column of Table 2) larger than that in germanate oxide glass. These results indicate that Er^{3+} ions are partly surrounded by F$^-$ ions in our glasses.

Fig. 2 shows the Raman spectra of un-doped glasses. The highest phonon frequency for the three glasses TP, GP and BP are located at 745, 783 and 1100 cm^{-1}, respectively. These high phonon bands result from stretching vibration of glass network structure Te–O–Te, Ge–O–Ge, and B–O–B linkages, respectively. The latter two values are both much smaller than those of their corresponding oxide glasses as displayed in the last two rows of Table 2 which can be explained as the destruction of the co-valent linkage cation–O–cation (such as Ge–O–Ge) with the addition of F$^-$ ions [26]. But for tellurite glasses, whether using PbO or PbF$_2$ as modifier, the highest phonon frequency barely changes because the Te–O bond is a typical ionic bond.

The room temperature upconversion spectra of all glasses with the same size of 10 mm × 10 mm × 2 mm under the same conditions such as optical setup, focalization point and illuminated cross-section, sample holder and emission and excitation slits width, etc. The spectra are shown in Fig. 3(a) and (b), respectively. The observed emissions correspond to transition of Er^{3+} ions from excited states to ground state.

Table 2
The phonon energy, refractive index n, and J–O intensity parameters in halide modified glasses

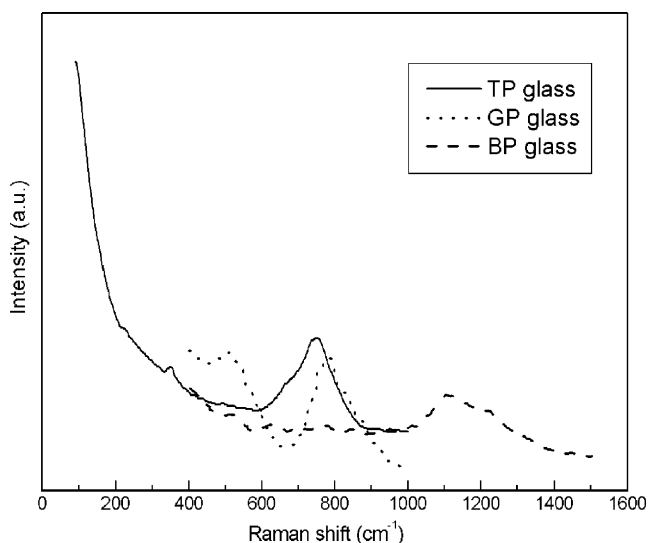| Sample	Phonon energy (cm^{-1})	Refractive index, n	Ω_2 (10–20 cm^2)	Ω_4 (10–20 cm^2)	Ω_6 (10–20 cm^2)
TPE (our work)	745	1.88	5.08	1.25	1.17
GPE (our work)	783	1.84	4.07	1.31	1.19
BPE (our work)	1100	1.60	3.4	1.50	1.19
50TeO$_2$–50PbO [22]	737	2.20			
GeO$_2$–PbO [23,24]	860	1.9–2.1	5.0	1.4	0.9
70PbO–30B$_2$O$_3$ [25]	1250	1.95			

Fig. 2. Raman spectra of un-doped glasses.

Fig. 3(a) shows the upconversion spectra of only Er^{3+}-doped glasses. The total emission intensities in the TPE glass is two times stronger than that in the GPE glass and no emission has been observed in BPE glass. According to Judd–Ofelt theory [21,22], the difference in absorption profiles of these glasses cannot account for that in their luminescent intensities. The effect of OH^- ions on emissions can also be neglected. Because the addition of F^- ions can effectively remove OH^- ions [27], and all glasses in our work have a very high concentration of F^- ions. In Er^{3+}-doped glasses, possible upconversion mechanisms are ground state and excited state absorption (GSA/ESA) and cross relaxation (CR) process between Er^{3+} ions [28]. The upconversion efficiency is determined by the lifetime of levels emitting light, which mainly relies on the phonon energy of the host according to energy gap law [15]. As mentioned in the analysis of Raman spectra, TPE glass has the lowest phonon energy and thus its emission is the strongest. Because the difference of phonon energy between germanate and tellurite glasses is not great, the emissions in TPE are only twice that in GPE glass. As
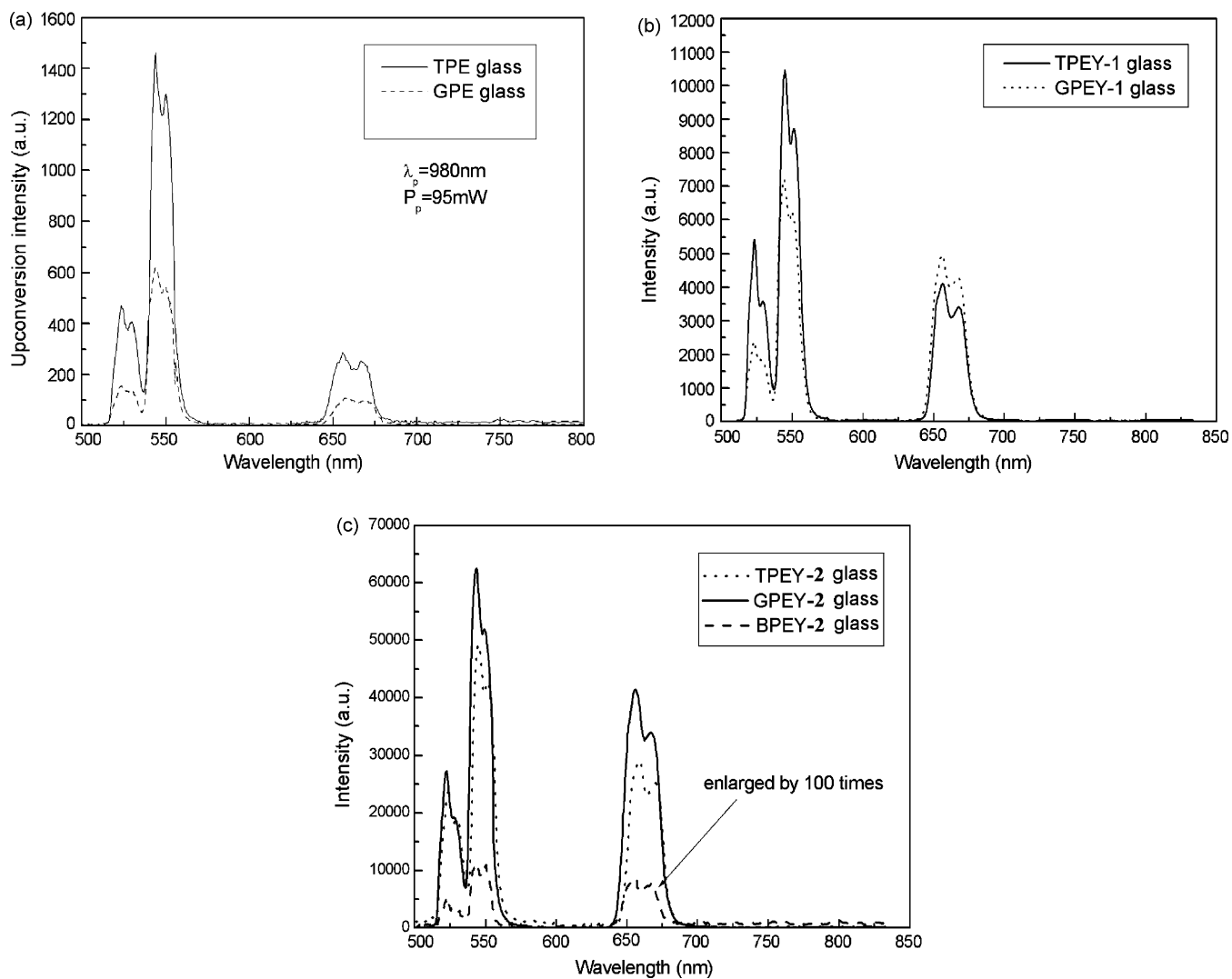

Fig. 3. (a) Upconversion spectra of Er^{3+}-doped glasses at room temperature for a fixed pump power of 95 mW at 980 nm. (b) and (c) Upconversion spectra of Yb^{3+}/Er^{3+}-codoped glasses (containing 1 mol Yb_2O_3) at room temperature for a fixed pump power of 95 mW at 980 nm. (c) Upconversion spectra of Yb^{3+}/Er^{3+}-codoped glasses (containing 2 mol Yb_2O_3) at room temperature for a fixed pump power of 95 mW at 980 nm.

for the BPE-2 glass, no emission has been observed because of its much higher phonon energy.

The intensity of the upconversion luminescence can be enhanced drastically by co-doping of sensitizer Yb^{3+} with Er^{3+} to the hosts. Upconversion spectra of Er^{3+}/Yb^{3+}-codoped glasses are shown in Fig. 3(b) and (c). It can be seen from Fig. 3(b) that the luminescence intensity gained almost one order of magnitude by co-doping of 2% of Yb^{3+} (1% Yb_2O_3) especially for green emission. By further increasing the content of Yb^{3+} from 2 to 4%, the luminescence intensity progressively increased 6–10 times. Comparing with a sample with no Yb^{3+}, the luminescence intensity increased by almost two orders of magnitude. Plenty of experiments verified that phonon energy is the dominant factor to influence the upconversion intensity but not a unique factor. If just comparing the luminescence intensities of sample TPEY-2 and GPEY-2, one may become confused because the intensity of GPEY-2 is greater than that of TPEY-2 instead. If comparing the intensities of all three kinds of the samples including BPEY-2, one may find that the phonon energy is still a dominant factor in influencing the upconversion properties. With the incorporation of Yb^{3+} ions, total green emissions have been enhanced by several or even 100 times than those in Er^{3+}-doped glasses because Yb^{3+} ion is an extremely effective absorber for 980 nm light [14]. We can also see that the red emission increases more than the green light.

Before further discussion, the ratio of the red to green (RRG) upconversion emission has been defined as the following equation:
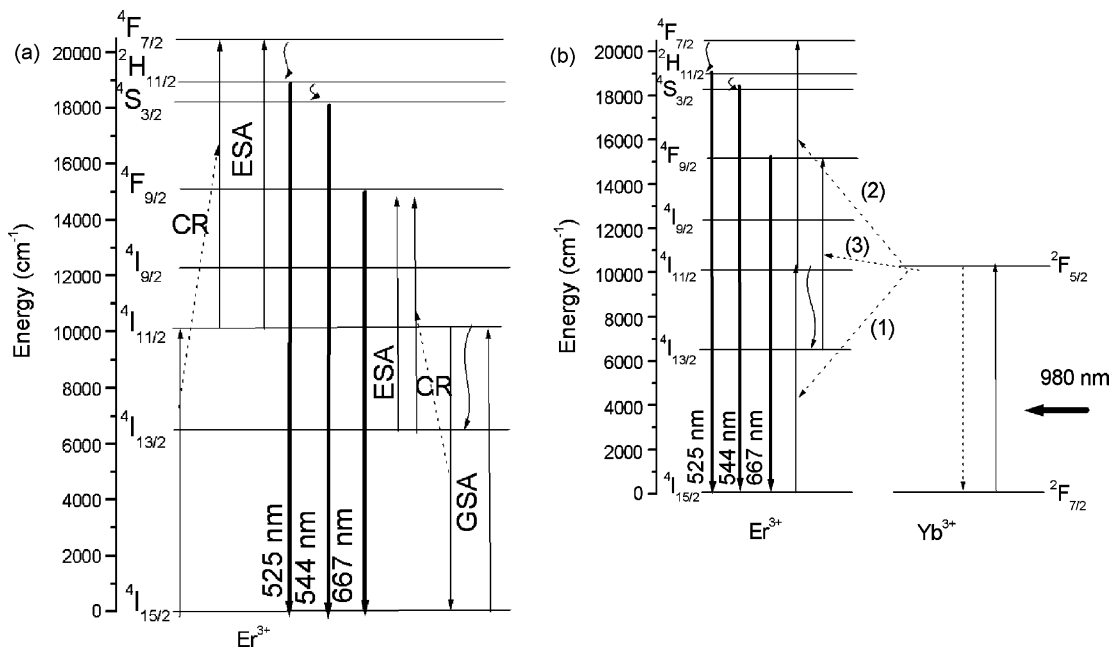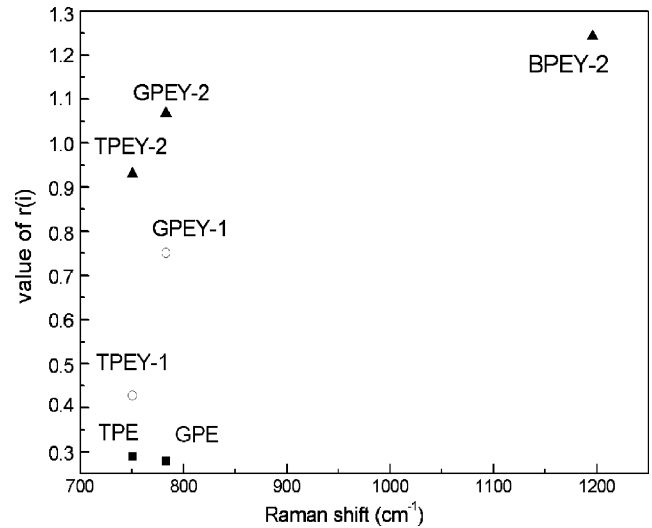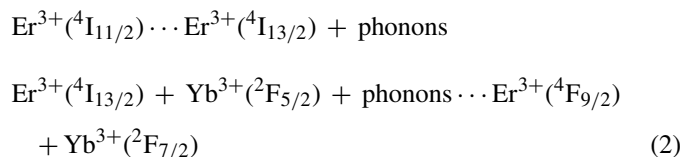
$$r(i) = \frac{Ir(i)}{Ig(i)} \quad (1)$$

Fig. 4. Emitting intensity ratio of the red band to the 544 nm green band.

where i is the code of the glass, $Ir(i)$ and $Ig(i)$, the integrated emitting intensities of the red and the 544 nm green bands, respectively. All the $r(i)$s are presented in Fig. 4. Values of r(TPE) and r(GPE), 0.29 and 0.28, are both much smaller than those in Er^{3+}/Yb^{3+}-codoped glasses. This indicates that contributions of the CR process between Er^{3+} ions shown in Fig. 5(a) to the red emission in Er^{3+}-doped glasses can be neglected. Meanwhile, $r(i)$ becomes apparently bigger with the increase of phonon energy in Er^{3+}/Yb^{3+}-codoped glasses. In Er^{3+}/Yb^{3+}-codoped glasses, the electronic population in $^4S_{3/2}$ level is accomplished through two successive energy transfers (1) and (2) from Yb^{3+} ions, shown in Fig. 5(b). They are both nearly res-

Fig. 5. (a) Simplified energy level diagram of Er^{3+} ion and possible upconversion luminescence mechanisms for Er^{3+}-doped glasses in our work. Solid straight lines with upward and down arrows indicate pumping and upconversion transitions, and radiative transitions, respectively; dot lines and wavy arrows denote energy transfer and non-radiative relaxation, respectively. (b) Simplified energy level diagram of Er^{3+}/Yb^{3+} ion and possible upconversion luminescence mechanisms for Er^{3+}/Yb^{3+}-codoped glasses. All the arrows have the same meanings as those in (a).

onant, about 10^{11} or 10^{12} s^{-1} [14], and independent of the host phonon energy. As a result, the green emissions are almost the same in Er^{3+}/Yb^{3+}-codoped tellurite and germanate glasses. But the emission in BPEY-2 is very weak because of the much higher phonon energy. For the red emission, electronic population in $^4F_{9/2}$ level can be accomplished through two channels. One is the multiphonon relaxation (MPR) process from $^4S_{3/2}$ which contributes little to electronic population in $^4F_{9/2}$ affirmed by the small $r(i)$s in Er^{3+}-doped glasses. The other possible channel for the electronic population in $^4F_{9/2}$ level is process (3) shown in Fig. 5(b), which can also be expressed in the following equation:

$$Er^{3+}(^4I_{11/2})\cdots Er^{3+}(^4I_{13/2}) + \text{phonons}$$

$$Er^{3+}(^4I_{13/2}) + Yb^{3+}(^2F_{5/2}) + \text{phonons}\cdots Er^{3+}(^4F_{9/2})$$
$$+ Yb^{3+}(^2F_{7/2}) \tag{2}$$

Er^{3+} ions in $^4I_{11/2}$ state can decay quickly to $^4I_{13/2}$. The second step is not resonant, and the energy mismatch is about 1557 cm^{-1}. This non-resonant process involves the participation of phonons [15]. As can be seen from Fig. 4, in Er^{3+}/Yb^{3+}-codoped glasses all $r(i)$s are bigger than 0.4 and $r(i)$ has an apparent tendency to increase with the increase of phonon energy. This dictates that phonon energy is one of the critical factors for the red luminescence of Er^{3+} in Er^{3+}/Yb^{3+}-codoped glasses. We can also note that $r(i)$ of GPEY-2 is much bigger than that of GPEY-1 which also happens to tellurite glasses. Similarly, our colleague's work obtained pure red color luminescence by increasing the ratio of Yb^{3+}/Er^{3+}. (Micro-structure and red upconversion luminescence of high concentration of rare-earth doped oxyfluoride crystallites, Yunxin Liu et al., to be published.)

4. Conclusions

Up to now, we have systematically analyzed the spectroscopic characteristics of a series of oxyfluoride glasses doped with Er^{3+} and codoped with Er^{3+}/Yb^{3+}. Several conclusions can be drawn.

(1) With the addition of F$^-$ ions, refractive index, phonon energy and Ω_2 of glasses decrease largely.
(2) Decreasing phonon energy can improve upconversion efficiency largely.
(3) Yb^{3+} ions can effectively enhance the total upconversion emitting intensities. One may find in Fig. 3(a–c) that the upconversion intensity was enhanced several to 100 times by co-doping Yb^{3+} ions.
(4) The addition of Yb^{3+} ions not only enhances the upconversion intensity but also raises the RRG. Phonons play

an important role in the upconversion process for the red emission.

Acknowledgements

References

[1] M. Tsuda, K. Soga, H. Inoue, A. Makishima, J. Appl. Phys. 85 (1999) 29.
[2] D.F. Sousa, L.F.C. Zonetti, M.v.V. Bell, R. Lebullenger, A.C. Hernandes, L.A.Q. Nunes, J. Appl. Phys. 85 (1999) 2502.
[3] P.V. dos Santos, E.A. Gouveia, M.T. de Araujo, A.S. Gouveia-Neto, A.S.B. Sombra, J.A. Medeiros Neto, Appl. Phys. Lett. 74 (1999) 3607.
[4] Li Feng, Jing Wang, Qiang Tang, Haili Hu, Hongbin Liang, Qiang Su, J. Non-Cryst. Solids 352 (2006) 2090.
[5] W.S. Tsang, W.M. Yu, C.L. Mak, W.L. Tsui, K.H. Wong, H.K. Hui, J. Appl. Phys. 91 (2002) 1871.
[6] A. Majchrowski, I.V. Kityk, E. Mandowska, A. Mandoski, J. Ebothé, T. Lukasiewicz, J. Appl. Phys. 100 (2006) 0531-01.
[7] B.R. Reddy, P. Vencateswarlu, Appl. Phys. Lett. 64 (1994) 1327.
[8] T. Catunda, L.A.O. Nunes, A. Florez, Y. Messaddeq, M.A. Aegerter, Phys. Rev. B 53 (1996) 6065.
[9] M.P. Hehlen, N.J. Cockroft, T.R. Gosnell, A.J. Bruce, Phys. Rev. B 56 (1997) 9302.
[10] M.A.P. Silva, Y. Messaddeq, V. Briois, M. Poulain, S.J.L. Riberiro, J. Phys. Chem. Solids 63 (2002) 605.
[11] Jianhu Yang, Liyan Zhang, Lei Wen, Shixun Dai, Lili Hu, Zhonghong Jiang, J. Appl. Phys. 95 (2004) 3020.
[12] A.S. Gouveia-Neto, E.B. da Costa, L.A. Bueno, S.J.L. Ribeiro, J. Alloys Compd. 375 (2004) 224.
[13] Hongtao Sun, Liyan Zhang, Junjie Zhang, Lei Wen, Chunlei Yu, Shixun Dai, Lili Hu, Zhonghong Jiang, Solid State Commun. 133 (2005) 781.
[14] Toru Miyakawa, D.L. Dexter, Phys. Rev. B 1 (1970) 70.
[15] Toru Miyakawa, D.L. Dexter, Phys. Rev. B 1 (1970) 2961.
[16] V. Nazabal, S. Todoroki, S. Inoue, T. Matsumoto, S. Suehara, T. Hondo, T. Araki, T. Cardinal, J. Non-Cryst. Solids 326–327 (2003) 359.
[17] Shiqing Xu, Zhongmin Yang, Guonian Wang, Shixun Dai, Junjie Zhang, Lili Hu, Zhonghong Jiang, J. Alloys Compd. 377 (2004) 253.
[18] Shiqing Xu, Guonian Wang, Junjie Zhang, Shixun Dai, Lili Hu, Zhonghong Jiang, J. Non-Cryst. Solids 336 (2004) 230.
[19] C.H. Kam, S. Buddhudu, J. Quant. Spectrosc. Radiat. Transfer 85 (2004) 1.
[20] S. Sanders, R.G. Waarts, D.G. Mehuys, D.F. Welch, Appl. Phys. Lett. 67 (1995) 1815.
[21] B.R. Judd, Phys. Rev. 127 (1962) 750.
[22] G.S. Ofelt, J. Chem. Phys. 37 (1962) 511.
[23] M. Wachtler, A. Speghini, K. Gatterer, H.R. Fritzer, D. Ajò, M. Bettinelli, J. Am. Ceram. Soc. 81 (1998) 2045.
[24] Z. Pan, D.O. Henderson, S.H. Morgan, J. Chem. Phys. 101 (1994) 1767.
[25] H. Ushida, et al., J. Alloys Compd. 377 (2004) 167.
[26] M.A.P. Silva, et al., J. Phys. Chem. Solids 62 (2001) 1055.
[27] Guonian Wang, Shixun Dai, et al., J. Lumin. 113 (2005) 27.
[28] Marie-France Joubert, Opt. Mater. 11 (1999) 181.